Biosensors and Bioelectronics 74 (2015) 981–988

Contents lists available at ScienceDirect

Biosensors and Bioelectronics

journal homepage: www.elsevier.com/locate/bios

A reusable optical biosensor for the ultrasensitive and selective detection of unamplified human genomic DNA with gold nanostars

Stefano Mariani [a], Simona Scarano [a], Jolanda Spadavecchia [b,c], Maria Minunni [a,*]

[a] Dipartimento di Chimica "Ugo Schiff", Università di Firenze, Via della Lastruccia 3-13, 50019 Sesto Fiorentino (FI), Italy
[b] Laboratoire de Réactivité de Surfaces, UMR CNRS 7197, Université Pierre & Marie Curie – Paris VI, Site d'Ivry – Le Raphaël, 94200 Ivry-sur-Seine, France
[c] Laboratoire CSPBAT UMR7244, UFR Santé, Médecine et Biologie Humaine, Université Paris 13, 74 rue Marcel Cachin, 93017 Bobigny, France

ARTICLE INFO

Article history:
Received 17 April 2015
Received in revised form
29 June 2015
Accepted 30 July 2015
Available online 1 August 2015

Keywords:
Reusable biosensor
Surface Plasmon Resonance imaging (SPRi)
Unamplified genomic DNA detection
Gold nanoparticles (AuNPs)
Gold nanostars (AuNSs)

ABSTRACT

A Surface Plasmon Resonance imaging (SPRi) based DNA sensors for the selective and ultrasensitive human genomic DNA detection, directly extracted from lymphocytes (bypassing PCR amplification), is reported. To achieve DNA detection, a rationally chosen star-shaped nanoparticle (NP), namely gold nanostar (AuNS), has been applied, for the first time, in a sandwich-like assay based on the selective capturing of specific DNA targets and the subsequent signal amplification by a secondary DNA probe linked to AuNS. The plasmonic profile, size and electric field enhancements at the star tips contributed to the maximization of plasmon coupling between LSPs and SPs as aimed for analytical signal magnification.

The system was first tested using short synthetic DNA target sequences and applied to DNA biosensing, lowering 610-fold the detection limit from 6.1 nM (without NSs labeling) to 10 pM (with NSs labeling). Then the biosensor was applied to genomic DNA samples, extracted from human lymphocytes and undergoing only to a simple ultrasonic fragmentation, lowering (~435 fold) the detection limit from 3.0 fM (without NSs labeling) to 6.9 aM (with NSs labeling). Thanks to the assay optimization, we proved that tuning the NSs surface coverage with DNA linked to nanoparticles is crucial not only for the increase of signals but also for the regenerability/reusability of the biosensor for tens of measurement cycles.

1. Introduction

One of the biggest challenges in the DNA affinity biosensing concerns the development of sensitive, selective, fast and cheap platforms for the direct detection of unamplified human genomic DNA directly extracted from biological samples and analyzed bypassing the PCR amplification step (Spoto and Corradini, 2012; Zanoli et al., 2012), in order to reduce the amount of employed reagents and the drawbacks ascribable to possible oligonucleotidic contamination (Shi et al., 2008).

Among the several transduction systems for DNA biosensing, Surface Plasmon Resonance imaging (SPRi) represents a progress in optical biosensing for multi-analyte, real-time, high-throughput and label free monitoring (Nelson et al., 2001; Scarano et al., 2010a; Spoto and Minunni, 2012; Steiner, 2004). SPRi exploits evanescent waves (EWs), generated by the total reflection of incident light, to monitor and localize bio-interactions (Homola, 2008). Bioreceptors (i.e. DNA probes) are bound on the sensing surface in micro-array formats and multi-arrayed signals and digital images of the interactions with analytes (i.e. DNA targets) are simultaneously recorded by a CCD camera. These features have opened new perspectives to multi- and parallel analyte DNA detection (Scarano et al., 2010a) with suitable applications in clinical analysis (Mariani and Minunni, 2014) and in particular for genetic and pharmacogenomic purposes (D'Agata and Spoto, 2013; Šípová and Homola, 2013).

Although commercially available SPRi platforms typically achieve detection limits in the nanomolar range by the label-free detection of synthetic DNA sequences (D'Agata and Spoto, 2013), the sensitivity required for biological samples (femtomolar/attomolar) is achievable by several approaches involving metallic nanoparticles (NPs), eventually coupled to enzyme signal amplification protocols. Alternatively to signal enhancing strategies, some attempt to directly measure the target sequence concentration in a label free manner, without the use of NPs or enzymes, has been recently reported by our group (Ermini et al., 2013; Mariani et al., 2015a) thanks to the fine tuning of all the parameters involved in the assay: probe design (i.e. in silico selection), sample pretreatment (i.e. optimized ultrasonication), and signal sampling and data

* Corresponding author.
E-mail address: maria.minunni@unifi.it (M. Minunni).

http://dx.doi.org/10.1016/j.bios.2015.07.071
0956-5663/

management. Among metallic nanostructures, AuNPs are the most employed in signal enhancement strategies (Szunerits et al., 2014) mainly for three reasons: (a) they have larger size than bio-analytes (i.e. DNA); (b) they generate a higher refractive index variation than commonly used dielectric materials and; (c) they provide optical coupling between electric field of localized surface plasmons (LPSs) and surface plasmons (SPs) further contributing to signal amplification (Spoto and Minunni, 2012). In 2004 Corn's group first reported a novel strategy for the picomolar and selective detection of the unamplified human BRCA1 gene coupling gold nanospheres (AuNSPs, 12–13 nm diameter) to enzymatic ligation reactions measurements on a thiolated DNA in microarray format. This strategy was further exploited also for single nucleotide polymorphisms (SNPs) discrimination associated with breast cancer and it appeared really attractive for potential parallel SNPs analysis (Li et al., 2006). More recently (2011), Spoto's group reported the attomolar detection of unamplified human β globin gene fragments, extracted from blood cells, by the development of a NPs-enhanced SPRi based on peptide nucleic acids (PNAs) sensor, coupling the high selectivity of PNAs probe to the amplification features offered by AuNSPs (20 ± 5 nm in diameter). The assay was tuned for the differentiation of SNPs, i.e. polymorphisms involved in β thalassemia (D'Agata et al., 2011).

Among the several NPs type embeddable in DNA based architectures (differing in material, size and shape) (Tan et al., 2011) the previous researches employed conventional Turkevich gold nanospheres (AuNSPs) (Daniel and Astruc, 2004) in a sandwich detection labeling strategy (Bedford et al., 2012), for easiness of making and of bio-functionalizing (gold/thiol chemistry). Very recently we eventually investigated nanoparticles properties in plasmonic nanoarchitectures with DNA by SPRi and showing how the optimal resonance condition achievable by the coupling between Surface Plasmons (SPs) and electric field of Localized Surface Plasmons (LSPs) occurs in presence of overlapping between the light source wavelength and the wavelength of LSPs excitation and that the contribution of this to %RV (Reflectivity Variation %, analytical signal monitored from the CCD SPRi instrument for lasting the bio-affinity interactions) is more crucial than NPs refractive index and size (Mariani et al., 2015b). At this purpose we report here for the first time a star-shaped gold NPs, i.e. gold nanostars (AuNSs), for the direct ultrasensitive detection of human genomic DNA by a sandwich-like assay based on SPRi. The increase in sensitivity derived by the use of these peculiar shaped NPs was recently reported in literature applied to DNA sensing application both by LSPR (Spadavecchia et al., 2013) (nanostars labeled to a secondary probe) and by conventional SPR using a graphene-modified surface (Zagorodko et al., 2014) (surface nanostructuring). Thus here for the first time, AuNSs were evaluated as signal amplifiers in SPRi-based DNA biosensing in a sandwich format and tested on a complex matrix, i.e. human genomic DNA. The selection of AuNSs as enhancing nanoparticles was based on the following considerations: (a) advantages of gold as reported above; (b) their big size ranging from 50–70 nm (Spadavecchia et al., 2013) and the fact that the sensitivity to surface density ($nm/\mu m^2$) of gold NPs increases with size (Špringer et al., 2014); (c) the plasmon peak at about 632 nm, really close to fixed monochromatic source wavelength of our instrument (635 nm) that could lead to an efficient plasmons coupling and in turn to an enhanced sensitivity (Mariani et al., 2015b); (d) the strong enhancement of the electric field and localized at the star tips that could couple more efficiently to SPs, providing a more penetrating evanescent wave with further sensitive plasmonic surface (Hao et al., 2007).

All these considerations supported the interest in exploring the capabilities of gold nanostars for developing ultrasensitive DNA biosensors. Here we thus report on SPRi-based DNA sensing first evaluating AuNSs amplification capabilities in comparison with conventional AuNSPs in a fine tuned DNA sandwich assay. The target DNA sequence belongs to the MDR1 gene, strategic in pharmacogenomics and clinical diagnostics since it is rich in SNPs which are related to many serious diseases such as colon and breast cancer (Marzolini et al., 2004, Mariani et al., 2015a).

The assay was first optimized on a short synthetic DNA target (Target, 84 mer) and then applied to the selective and ultrasensitive MDR1 gene detection in human DNA samples (by-passing the PCR step) directly extracted from lymphocytes and subjected to an efficient ultrasonic fragmentation protocol (Ermini et al., 2013, Mariani et al., 2015a). We prove here that by the use of AuNSs not only the ultrasensitive detection is successfully achievable, but also that by the tuning of the optimal DNA probe labeling concentration the affinity interactions are well reversible, making the DNA sensor regenerable and reusable for multiple measurements on the same biochip. This finding represents an improvement compared to the state of the art of ultrasensitive genomic DNA detection with AuNPs, where no data about regeneration and reusability were so far reported in genomic DNA.

2. Experimental section

2.1. Oligonucleotides, salts reagents and buffers

Synthetic oligonucleotides (probes and target) were purchased from Eurofins MWG Operon (Ebersberg, Germany) and have the following sequences: Probe1 (thiolated) 5′ HS-$(CH_2)_6$-GTC-ACT-GCC-TAA-TGT-AAG-TCT-C 3′ (22 mer); Target 5′ GAG-ACT-TAC-ATT-AGG-CAG-TGA-CTC-GAT-GAA-GGC-ATG-TAT-GTT-GGC-CTC-CTT-TGC-TGC-CCT-CAC-AAT-CTC-TTC-CTG-TGA-CAC-CAC 3′ (84 mer); EProbe (Enhancing Probe, thiolated) 5′ HS-$(CH_2)_6$-GTG-GTG-TCA-CAG-GAA-GAG-ATT 3′ (21 mer), CProbe (Control Probe, thiolated) 5′ HS-$(CH_2)_6$-GAG-GGC-GAT-GCC-ACC-TAC (18 mer).

The Target sequence was selected from the MDR1 human gene (or ABCB1) and the Probe 1 was selected by Oligowiz 2.0 (Wernersson et al., 2007) as the best performing probe in terms of selectivity towards the gene. Details of the Probe1 selection are reported in a previous study (Ermini et al., 2013).

An aqueous solution (pH=7.4) of potassium phosphate monobasic (KH_2PO_4, 20.0 mM), sodium chloride (NaCl, 300 mM), ethylenediaminetetraacetic acid (EDTA, 0.1 mM) was used as PBS running buffer while a potassium phosphate monobasic (KH_2PO_4, 1.0 M) aqueous solution (pH 3.8) was used for the Probe1 and CProbe immobilization. 11-mercapto-1-undecanol (MU, 1.0 mM) and 6-mercapto-1-hexanol (MCH, 1.0 mM) in aqueous solution were used for gold chip surface passivation. Protoporphyrin IX (PP, 95%), cetyltrimethyl ammonium bromide (CTAB), ethanol (EtOH), tetrachloroauric acid ($HAuCl_4$), silver nitrate ($AgNO_3$), sodium borohydride ($NaBH_4$), and ascorbic acid were used for gold nanostars synthesis while tetrachloroauric acid ($HAuCl_4$) and trisodium citrate were used for gold nanospheres synthesis. All the previous salts and reagents were purchased from Sigma Aldrich (Milan, Italy). Polydimethylsiloxane (PDMS, Sylgard 184 Silicone Elastomer Kit, Dow Corning, UK) was employed for the microwelled mask making (Scarano et al., 2010a). Human genomic DNA was purchased from Novagen (Piacenza, Italy) and used for the real sample testing. The commercial sample consisted of a pool of DNA extracted from human lymphocytes from different individuals, reported to be at least 90% greater than 100 kbp in size and purified for the elimination of free of contaminating RNA, protein and restriction enzymes. Solutions were prepared in MilliQ water and filtered using vacuum filter cups (Millipore E express plus, 0.22 μm) and/or syringe filters (Puradisc, cellulose acetate, 0.2 μm from Whatman GmbH, Dassel, Germany) before use.

2.2. Gold nanostars and gold nanospheres synthesis

Gold nanostars (AuNSs) were synthesized by a seed-mediated method previously reported (Spadavecchia et al., 2014) where Protoporphyrin IX (PP) was added both in the seed synthesis and in the growth solution. Gold seeds were prepared by adding PP into the reaction mixture as follows: 5 mL of 0.20 M CTAB were added to 5 mL of 6.3×10^{-4} M PP in EtOH/H_2O (3/2) solution, at 27 °C under stirring conditions; 5.0 mL of a 2.5×10^{-4} M $HAuCl_4$ in aqueous solution and 0.6 mL of ice-cooled $NaBH_4$ (0.01 M) were then added. The so-prepared solution was centrifuged at 15,000 rpm for 10 min. The supernatant was discarded and the residue was re-dispersed in an equivalent amount of MilliQ water. Growth solution was prepared by adding 5 mL of 0.20 M CTAB to 5.0 mL of 6.3×10^{-4} M PP and $AgNO_3$ (0.25 mL; 4.0×10^{-3} M) and stirring for 10 min. After this time, 5.0 mL of $HAuCl_4$ (1.0×10^{-3} M) were transferred to the mixture, and 70 μL of ascorbic acid (8.0×10^{-3} M) added. Finally, 12 μL of gold seeds solution were added in the growth solution. AuNSs were centrifuged at 8000 rpm for 20 min and analyzed by UV–vis spectroscopy and transmission electron microscopy (TEM). NSs concentration was estimated from the total amount of $HAuCl_4$ in the growth solution (1×10^{-3} M in 15 mL (final volume)), the Au density (density 19.30 g/cm^3), and sketching the shape of the nanostars to a sphere of 30 nm in radius. The estimated NSs concentration resulted $\sim 3.0 \times 10^{10}$ NSs/mL. Fig. 1 shows the TEM image (a and b) and the LSPR spectrum of AuNSs after the synthesis (c).

TEM images confirmed that the star-shaped NPs are characterized by variable sizes from 50 to 70 nm. The LSPR AuNSs spectrum displayed a plasmon band, due to the rather short branches transition at 632 nm, closely located near the 635 nm source wavelength used by the SPRi Lab$^+$ (Horiba).

Gold nanospheres (AuNSPs) were synthesized accordingly to the protocol described by Turkevich (Daniel and Astruc, 2004). 5 mL of a 1.0 mM $HAuCl_4$ solution were added in a flask under magnetic stirring with MilliQ water. The solution was brought to boiling and 0.25 mL of a 40 mM citrate solution was added. AuNSPs concentration was again estimated from the total amount of tetrachloroauric acid (9.85×10^{-4} g) used for the synthesis, and the total aqueous volume (25 mL). Nanospheres dimension was estimated by SEM microscopy (ø$\sim 24 \pm 3$ nm) and gold density (19.30 g/cm^3) (Mariani et al., 2015b). As a result, the theoretical concentration resulted 2.8×10^{11} NPs/mL (Mariani et al., 2015b).

2.3. Labeling DNA probe to gold nanospheres and nanostars

Gold nanospheres (AuNSPs) and gold nanostars (AuNSs) were covalently bound to 5′-thiol capped 22 mer EProbe accordingly to the protocol described by Mirkin et al. (1996), testing different NPs/EProbe ratios to optimize the conditions, as discussed in Section 3 paragraph.

100 μL of each NPs dispersion were first centrifuged at 10,000 rpm for 5 min and the supernatant was discarded to remove the excess of stabilizing agents present in the synthesis solution. NPs were then resuspended in 95 μL PBS running buffer (pH=7.4). 5 μL of 5.0 μM thiolated EProbe were added to both dispersions to obtain a maximum achievable 250 nM Eprobe concentration anchored to nanoparticles in 100 μL of dispersion. After 16 h of incubation in dark room, the dispersions were centrifuged at 10,000 rpm for 10 min, the supernatant containing the unbound EProbe was discarded, and the NPs linked to EProbe were finally resuspended in 100 μL of PBS buffer.

2.4. Biochip preparation

SPRi-Biochips™ (Horiba, France) glass prisms coated with a

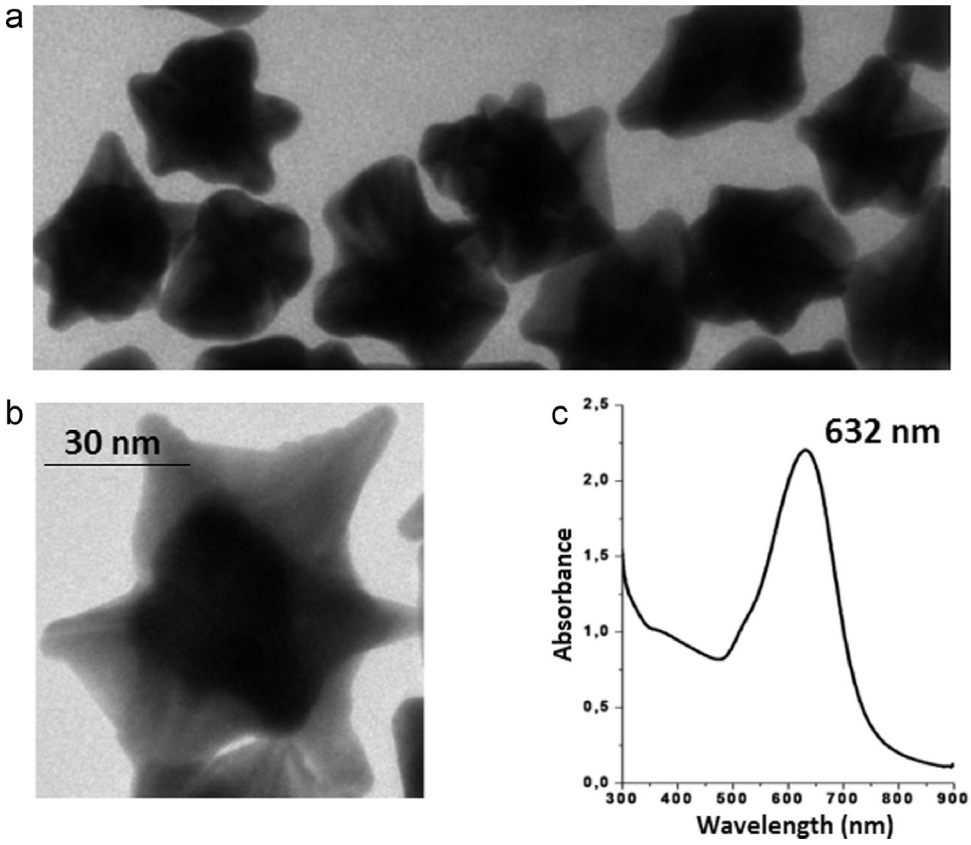

Fig. 1. (a, b)TEM image of gold nanostars (AuNSs); (b) LSPR spectrum of AuNSs.

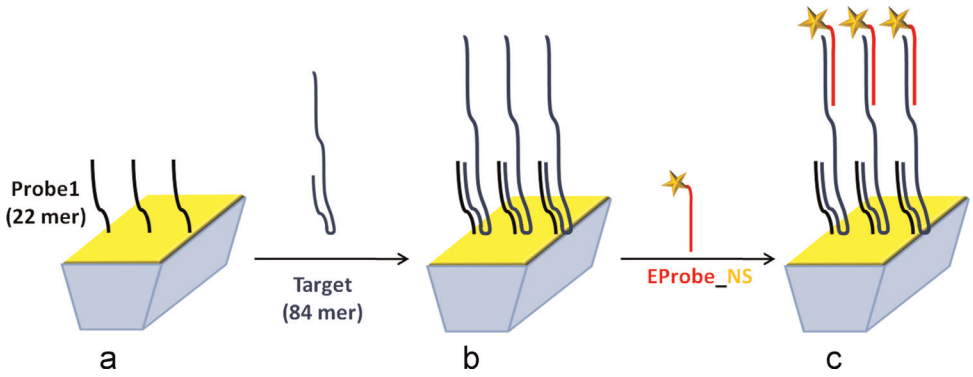

Fig. 2. Sketch of the assay with synthetic Target. (a) Probe1 (black) is immobilized as capturing probe to the gold chip surface exploiting the thiolic functionalization. (b) Target (blue) complementary to Probe1 is hybridized to the biochip surface. (c) EProbe_NS (red) is hybridized to the preformed hybrid to achieve signal enhancement. (For interpretation of the references to color in this figure legend, the reader is referred to the web version of this article.)

thin gold layer (50 nm) were used for the DNA sensor preparation. 10 μM of thiolated Probe1 and CProbe were first dissolved in 20.0 mM KH_2PO_4 aqueous solution pH 3.8 and then spotted in a microwelled PDMS mask overlapping the bare gold prism (0.8 μL in each microwell). After 48 h of incubation in a moist chamber for the covalent anchoring of thiolated DNA probes on the gold surface, the PDMS mask was removed and the biochip was immersed in the thioalcholic aqueous solution (1.0 mM MU and MCH) for 16 h to achieve surface passivation. This last step was carried out only for the synthetic Target detection while it was bypassed in Human Genomic DNA detection accordingly to a previous optimization (Ermini et al., 2013).

2.5. Surface Plasmon Resonance imaging measurements

Analytical signals of DNA/DNA affinity bindings were recorded as Reflectivity Variation % (%RV) by SPRi-Lab$^+$ from Horiba Scientific (France). The whole instrumental setup was previously reported by Scarano et al. (2010a). 100 μL of DNA targets were first dissolved in PBS running buffer and then injected through a Rheodyne valve in the fluidic system. For synthetic Target, a PBS running buffer flow of 6.0 μL/min was used and the affinity interaction for 30 min. For the pre-treated human genomic DNA, the PBS running buffer flow was 1000-fold increased (6.0 mL/min.) during injection of the sample, accordingly to previous researches (Ermini et al., 2013; Mariani et al., 2015a), and then promptly lowered to 6.0 μL/min, lasting the affinity interaction for about 30 min. Enhancing Probe1 labeled to AuNSs (EP_NSs) was added on the preformed hybrid at a flow rate of 30 μL/min. 10 mM NaOH (300 μL/min) solution was used as regeneration solution (i.e. dsDNA hybrids dissociation) after each measurement cycle for 20 s. %RVs reported in this work were all averaged on 3 replicates, and each %RV deriving from a replicate was sampled and averaged from nine (3 × 3) circular Regions of Interests (ROIs, 1.8 mm diameter) (Scarano et al., 2010b) inscribed in each spot (1.0 mm) of the array biochip carrying immobilized Probe1 and CProbe sequences. %RVs recorded from Probe1 and CProbe spots were subtracted of the %RV recorded on blank spot (bare gold, B) during the injections. Affinity interactions were monitored at room temperature (20 °C).

2.5.1. UV/vis measurements

Perkin-Elmer Lambda UV/vis 950 spectrophotometer was used for the absorption spectra acquisition of AuNSs in plastic cuvettes with an optical path of 10 mm. The wavelengths range was 400–700 or 400–1100 nm.

2.5.2. Transmission electron microscopy (TEM)

JEOL JEM 1011 TEM was used to record microscopic images of AuNSs operating at an accelerating voltage of 100 kV. TEM images were taken after separating the gold nanoparticles from the CTAB surfactant by 21 min at 11,000 rpm centrifugation, supernatant was discarded while AuNSs were re-suspended in PBS buffer solutions (pH 7.4), placed on a carbon-coated copper grid and dried at room temperature.

3. Results and discussions

3.1. Assay optimization: DNA probe labeled to nanostars and synthetic target

A sandwich-like assay was designed as follows: Probe1 was immobilized on the gold sensing surface as capturing probe selective for the Target analyte (complementary to Probe1), while the EProbe_NS (complementary to a different region of the target) was added to the preformed Probe1/Target hybrid to improve % RVs recorded.

In Fig. 2 the sketch of the assay is reported. The Target sequence was selected from the MDR1 fragment, strategic in pharmacogenomics and clinical diagnostics (Marzolini et al., 2004, Mariani et al., 2015a).

The analytical performances of the biosensor were first assayed on the synthetic Target (84 mer) to evaluate the repeatability of the affinity interaction with Probe1 and the detection limit of the system. As result, a linear range of calibration was recorded between 0 and 100 nM with a good linear correlation $R^2=0.997$, while between 100 nM and 1.00 μM a saturation trend occurs (Fig. A1a in Electronic Supplementary Information, ESI). The %CV averaged for all the calibration points, for the three replicates, was 8.7% emphasizing the good repeatability of the measurements. Then the detection limit from the calibration curve sensitivity (0.015 %RV/nM) and the 3.3-fold instrumental noise ($S=0.092$ % RV, $N=0.028$ %RV) was evaluated, obtaining a DL=6.1 nM in agreement with the nanomolar detection limits reported in literature for SPRi based DNA sensing with synthetic targets without enhancing strategies and/or instrumental or biochip advancements (D'Agata and Spoto, 2013). The binding resulted well regenerable through the injection of a chaotropic agent (NaOH, 10 mM in aqueous solution at flow rate 300 μL/min), as reported by the sensorgram in ESI Fig. A1c.

Afterwards the effect of the EProbe_NS adduct in enhancing the signals by the secondary hybridization was evaluated in sandwich-like format. To this aim, the EProbe_NS was added in sequence (Fig. 2) and the effect of its addition was evaluated in terms of DL limit lowering.

Aiming at maximizing the hybridization efficiency and the magnitude of %RV, the EProbe/NSs ratio was optimized. Three different EProbe/NS ratios were tested, *i.e.* 2×10^3, 2×10^4 and 2×10^5. These values should be however considered as indicative, *i.e.* theoretical and approximate values since after the incubation NSs and EProbe mixtures were centrifuged to remove eventual unbounded EProbe. Such ratios have been intentionally chosen higher than those reported in literature for different NPs in sandwich like DNA assays (hundreds of probe for NP) (Zanoli et al., 2012) in order to explore the effect of increasing the EProbe surface area density on the NPs stability, making the NSs more dispersed in solution, thanks to nucleic acid electrostatic repulsion, and then less subjected to aggregation and collapse at chip surface, in order to promote a more efficient regeneration. The signals recorded after the addition of the EProbe_NS at different ratios were: 1.164 ± 0.333, 2.389 ± 0.155 and 0.782 ± 0.070 %RV for 2×10^3, 2×10^4 and 2×10^5 EProbe/NSs, respectively. Therefore, the 2×10^4 oligonucleotidic surface coverage allowed the best hybridization efficiency and was further used for the ultrasensitive detection of the Target sequence in human genomic DNA. In presence of lower surface EProbe density (2×10^3 EProbe/NSs), a random interaction (%CV=29%) was recorded, probably due to gold NSs collapsing and subsequent lowering of the recorded signal on Probe1. At 2×10^5 EProbe/Ns ratio was recorded the lowest %RV (0.782%RV), probably due to the high steric hindrance of EProbe strands on the nanostars surface that affects the DNA/DNA binding efficiency.

In Fig. 3 the sensorgram of the affinity interaction with 250 nM synthetic Target (a) and the subsequent EProbe/NSs secondary binding (b) is reported, together with the digital images recorded at the corresponding steps of the sandwich-like strategy.

The sensorgram emphasized that the interaction with the complementary Target occurred selectively only on the Probe1 (step (I)), while on CProbe 'C' and on the bare gold surface no signal was observed. When the EProbe_NS adduct was injected on the pre-formed hybrid to enhance the signal, a huge variation in reflectivity is obtained, as expected (step (b)). However, this variation involved with a lesser extent the control spot 'C'. In particular, %RV~11% was observed on the Probe1 while ~2% on CProbe. This behavior could be elicited by the establishment of electrostatic interactions between the partial positive charge of nanostars and the negatively charged spots and bare gold. Positive residual charges on AuNSs could result from the CTAB, the cationic surfactant used as stabilizer to maintain stable the NSs dispersion and to avoid their collapse. Despite AuNSs were centrifuged and re-suspended in PBS buffer before their functionalization with EProbe, some residual CTAB could be left from the previously centrifugation protocol optimized for an efficient NSs washing step

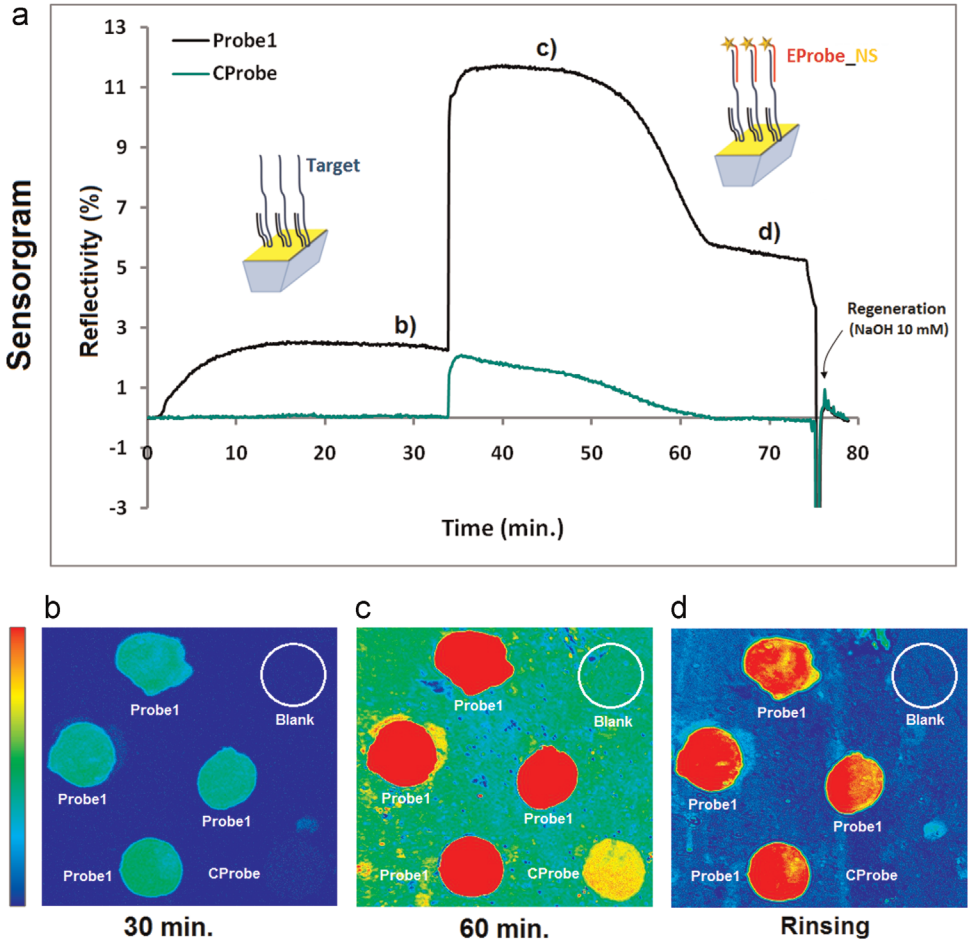

Fig. 3. (a) Sensorgram (Reflectivity% vs time) of 250 nM Target recorded on Probe1 (capturing probe, black curve of sensorgram) and on CProbe spots (Control Probe, green curve of sensorgram). Above the black Probe1 sensorgram are reported the sketches of the assay with synthetic Target (84 mer), hybridizing on Probe1, and of the subsequent addition of the EProbe_NS performed to achieve signal enhancement. The relative digital images recorded for Probe1 (5 replies for chip), CProbe and Blank spots at the different steps are reported in (b) (c) and (d). In (b) is reported the image after 30 min from Target injection; in (c) is lasted the image after the injection of EProbe_NS, in (d) is monitored the rinsing step where the excess of EProbe_NS is removed. Blue-sky blue colors means no interaction while colors ranging from green to red means increasingly efficient bio-affinity interaction (in relation to the color scale bar) causing an increasingly reflectivity variation % (% RV). (For interpretation of the references to color in this figure legend, the reader is referred to the web version of this article.)

without NPs collapse. As reflection, the interaction of EProbe_NS with the negatively charged Probe1 could be governed not only by the specific DNA/DNA recognition (base pairing) but also by the electrostatic force between cationic CTAB and the biochip surface. This hypothesis is supported by the evidence that this interaction is weak and quickly fades off under buffer flushing (30 μL/min). After the flushing step, the remaining signal is essentially ascribable to the sole base pairing on Probe1, whereas negligible signal is detectable on the CProbe and on bare gold surface (step (c)). To assure system selectivity, %RVs of all the reported measurements were thus sampled after the flushing step, under the unspecific contribution became zero. Finally, the hybrid was completely dissociated and the baseline instantly recovered by the injection of a chaotropic agent (10 mM $NaOH_{aq}$, 300 μL/min, 30 s), making the DNA sensor regenerable for subsequent measurements. This result is in general not obvious when working with metallic nanostructures, since possible unspecific interactions and NPs collapsing could lead to supra-molecular clusters, which poison the surface, preventing any surface reuse. The possibility of a fast surface recovery represents a main requisite in SPR-based bioassays, not only to limit costs and preparation times, but also to rise up the Surface Plasmon Resonance imaging-based sensing applicability to routine analyses. This result represents thus an important innovation compared to the current literature where chips are reported for only single use.

To evaluate the improvement obtained with the use of gold nanostars, the signal amplification obtained by using the EProbe_NS adduct was compared to that obtained by conventional gold nanoparticles (nanospheres, AuNSPs). The AuNSPs were modified with EProbe at the same theoretical EProbe/Ns surface density previously optimized for nanostars, to equalize contingent differences in steric hindrance of EProbe strands on the nanoparticle surface.

As a result, when the EProbe_AuNSPs adduct (nanospheres) is applied, a signal ~5-fold lower (0.463 ± 0.032 %RV) than the one recorded with EProbe_NS (nanostars, 2.389 ± 0.155 %RV) was obtained. This finding confirms that, among gold nanostructures potentially useful for this aim, a rational selection of size and shape to be employed is a key feature to maximize the secondary signal enhancement. The 5-fold improvement of the signal obtained with nanostars could be attributed to various positive contributions: the increase of the particle size (AuNSPs, ~24 nm; AuNSs ranging from 50 to 70 nm) as recently reported also by Homola's group (Špringer et al., 2014); the more efficient wavelength overlapping between source wavelength (635 nm) and AuNSs plasmon peak (~632 nm), causing a more efficient plasmons coupling with a collateral improvement of the sensitivity (Mariani et al., 2015a); a more a stronger plasmon coupling between AuNSs and SPs, elicited by the highly enhanced electric field at the star tips (Hao et al., 2007).

After the previously reported optimization we tested analytical performances at decreasing Target concentration from 1.00 μM to the lowest detectable concentration in the sandwich-assay with AuNSs. The results were reported in Fig. 4.

In Fig. 4a the overall %RV signal obtained for each concentration point is split in the two different contributions of the sandwich-like assay, *i.e.* the first elicited by the binding of the Target and the second one by the secondary addition of the EProbe_NS adduct. A sigmoidal dose response was observed both for Target and for the amplification with EProbe_NS, in agreement with previously reported experiments of signal enhancing with AuNSs in LSPR-based DNA sensing (Spadavecchia et al., 2013). In Fig. 4b was reported the zoomed graph (from Fig. 4a) below 10 nM Target concentration, in which no significant primary signals were recorded. This result is in line with the calculated detection limit for the Target, as extrapolated from the relative calibration curve (Fig. A1b in ESI), resulting 6.1 nM from the S/N ratio (S/N = 3.3). On the contrary, significant %RV signals were recorded with the addition of EProbe_NS binding at these concentrations, confirming that the use of nanostars modified with the secondary probe allows an improvement of the system experimental DL from 6.1 nM to 10 pM (0.097 ± 0.047), i.e. 610-fold lower than the DL recorded by the direct detection in absence of the EProbe_NS secondary binding.

This strategy opened a new interesting perspective in the ultrasensitive detection of unamplified DNA fragments from blood cells, as further tested in this work.

3.2. Hybridization experiments with human genomic DNA

The previous section of the work was conducted with a relatively short sequence (84 mer), selected in silico (Ermini et al., 2013) able to hybridize two different probes (Probe1 and EProbe_NS) mapping in different sites, as mimicking model for more complex and longer fragments possibly present in real matrices, such as DNA extracted from biological specimens, which could be the best candidate for system application to clinical molecular diagnostics.

Indeed the system was finally tested on commercially available

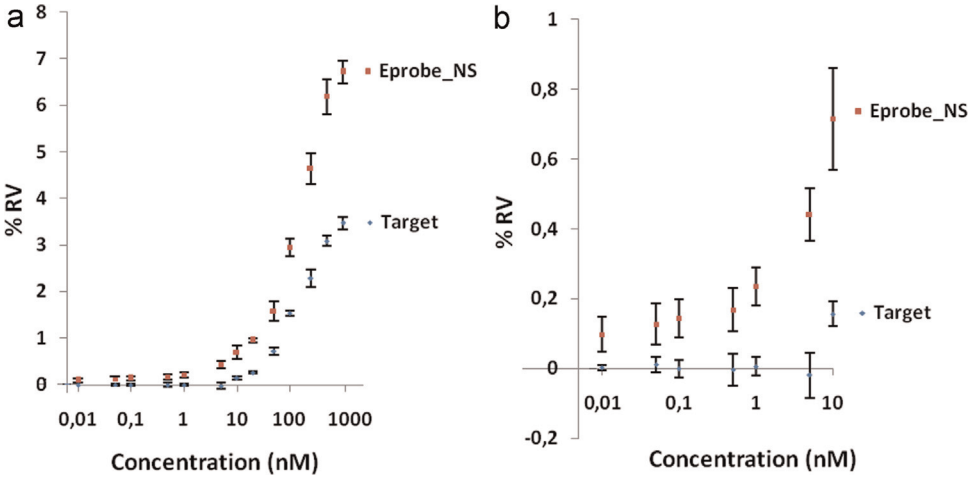

Fig. 4. (a) Reflectivity Variations (%RVs) recorded at decreasing Target concentration from 1.0 μM to 10 pM, directly compared to %RVs obtained by the sandwich-like strategy, i.e. the injection of EProbe_NS; (b) Zoom in of (a), between 10 nM and 10 pM. Both graphs are reported in semi-logarithmic scale, and %RV signals obtained for each concentration point are split in the two different contributions of the sandwich-like assay.

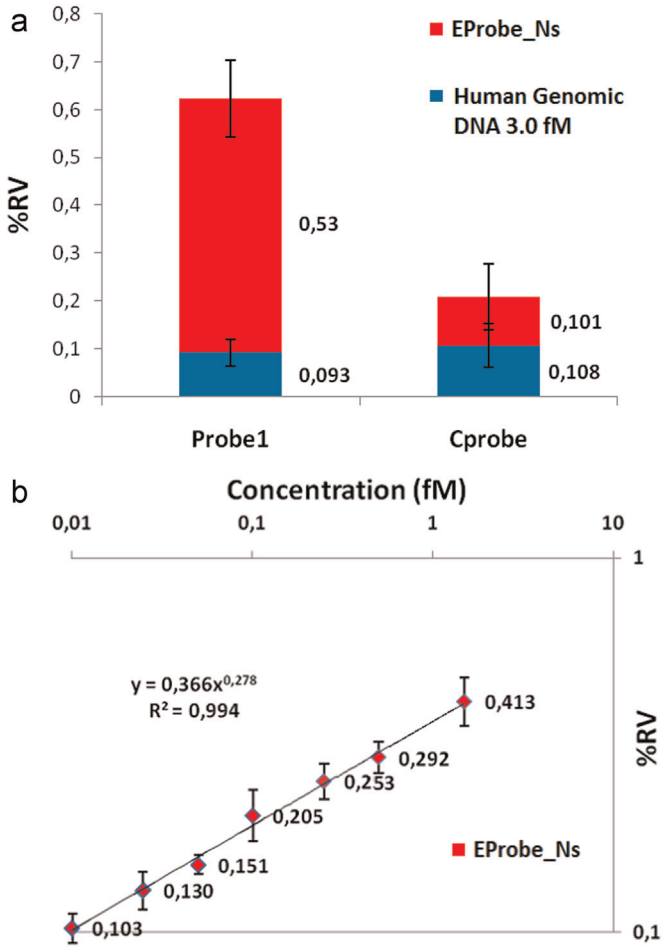

Fig. 5. (a) Bar plot for the selectivity evaluation of the EProbe_NS binding through the simultaneous hybridization of 3.0 fM genomic DNA on Probe1(capturing probe) and CProbe (control probe); (b) Plotting %RVs of EProbe_NS addition *vs* genomic DNA ranging from 1.5 fM to 10 aM in a logarithmic diagram.

human genomic DNA extracted from donors' pool lymphocytes. The DNA was only subjected to a fast and simple pretreatment consisting of ultrasonic fragmentation, which ensures the generation of long fragments (~10,000÷20,000 bp), and followed by thermal denaturation (Ermini et al., 2013), both of them strategic for the femtomolar detection of genomic DNA sequences (Ermini et al., 2013; Mariani et al., 2015b).

Pretreated genomic DNA samples were then assayed by the same sandwich-labeled strategy, previously reported in Fig. 2 for the synthetic Target, exploiting the EProbe_NS adduct as signal enhancer. We first evaluated the selectivity of the assay with a 3.0 fM human genomic DNA sample concentration (Fig. 5a), and then the logarithmic dose-response trend to evaluate the experimental detection limit (Fig. 5b).

As reported in Fig. 5b, after the injection of 3.0 fM human genomic DNA significant %RVs both on Probe1 (0.093 ± 0.028 %RV) and on control CProbe (0.108 ± 0.048 %RV) were recorded. This result was expected since CProbe might randomly hybridize to genomic DNA sequences (Mariani et al., 2015b). The randomicity on CProbe was indeed suggested by the %CV (~44%), higher than the one reported for Probe1 (~30%). The selectivity of Probe1 binding versus the Target sequences was further assessed by the secondary binding of EProbe_NS to the hybrid; indeed we proved that only on Probe1 the secondary hybridization was significant (0.530 ± 0.081 %RV, %CV~15%), confirming that only this probe selectively hybridizes to the complementary MDR1 fragments. Therefore, on the CProbe the secondary interaction could not be considered selective (0.101 ± 0.070 %RV), confirming the randomicity of the genomic hybridization as suggested by the really high %CV~70%.

Once assessed the selectivity of the interaction, we tested the analytical performances of the assay at decreasing concentrations of human genomic DNA. As reported by the logarithmic diagram of the EProbe_NS addition in Fig. 3c a linear dose response was shown between 1.5 fM and 10 aM genomic DNA samples. As result by the recorded mathematical correspondence ($y=0.366x^{0.278}$, or after linearization $y=0.278x-0.436$, $R^2=0.994$) and by the 3.3-fold instrumental noise ($S=0.092$ %RV, $N=0.028$ %RV) an instrumental DL=6.9 aM was found, being ~435-fold lower than those without EProbe_NS, proving the suitability for applications to ultrasensitive and selective detection of target sequences directly in genomic DNA, by avoiding the classical pre-amplification step by PCR.

Furthermore, we demonstrate that the interaction with these nanoparticles is well reversible (see sensorgram in Fig. 6) by the simple injection of 10 mM NaOH, making the biosensor reusable for tens analyses of different samples on the same biochip.

Effectiveness and effects of the regeneration were estimated after 30 measurement/regeneration cycles on DNA samples (with synthetic and extracted genomic samples). To this aim, the Target (synthetic, 84 mer) was used as indicator both for the surface regeneration effectiveness and for its possible degradation. SPRi signal (%RV) obtained by injecting 250 mM Target on Probe1 at the beginning of the experiment was taken as 100% of the recordable signal and finally compared with the same one obtained after 30 measurement/regeneration cycles. The hybridization signal recorded at the 30th measuring cycle was 2.148 ± 0.202 %RV, not significantly diverging from the same one recorded at the first measurement cycle of the experiment, i.e. 2.333 ± 0.186 %RV (*t*-student test, 3 replicates, significance level $p=5\%$).

The biosensor regenerability is an important task which could eventually contribute to decrease the analysis costs (especially when expensive chips are employed as in SPR-based sensing), among others advantages.

These achievements are the results of several rational approaches applied to the development of the whole bioassay: the rational selection of the capturing probe (Probe1) ensures the selectivity of the affinity interaction; the functional choice of the nanoparticles (material, size, and shape) proves that gold nanostars allow a 5-fold signal enhancement compared to the mostly used Au nanospheres as SPR couplers (2.389 %RV *vs* 0.463 %RV, respectively for AuNSs and AuNSPs); the optimization of the nanostars coating with EProbe allows finding the best compromise between an efficient coverage of NSs to avoid collapse on the

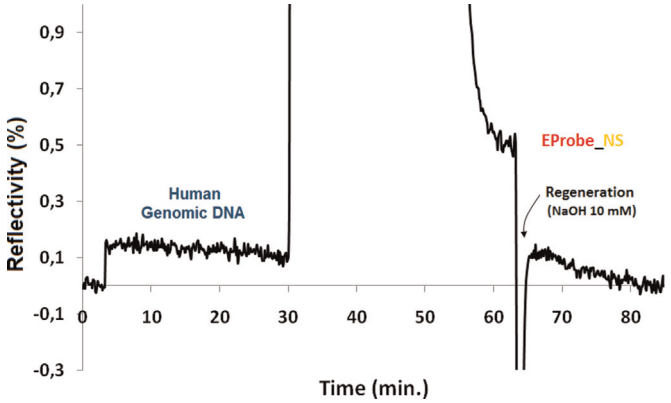

Fig. 6. Sensorgram (Reflectivity% *vs* Time, black line) recorded on capturing probe (Probe1) of the affinity interaction with 3.0 fM human genomic DNA and of the subsequent hybridization with EProbe_NS on the preformed hybrid (after the rinsing step).

biochip surface (with subsequent no reusability of it) and a reduced steric hindrance among EProbe strands (with subsequent low binding efficacy).

4. Conclusions

In this research we developed a selective, ultrasensitive (down to 10 aM) and regenerable/reusable (over 30 measurement cycles) DNA-based sensor, by SPRi optical transduction, for the detection of unamplified human genomic DNA extracted from lymphocytes. This goal was achieved by using emerging gold nanoparticles, i.e. gold nanostars (AuNSs). We proved that the analytical performance of a direct detection can be strongly improved, in terms of DLs, by a sandwich-like assay based on the selective capturing of the genomic target and the subsequent signal amplification using a complementary secondary DNA probe labeled with gold nanostars (AuNSs). For the first time, this kind of NPs are employed for human genomic DNA biosensing by SPRi, pointing out that the rational choice of their size, shape and plasmonic profile can be critical for the maximization of the result, as we proved by the comparison with conventionally employed gold nanospheres (AuNSPs).

We also assessed that the tuning of the NSs surface coverage with the secondary probe (EProbe) is crucial not only for the increase of signals but also for the regenerability/reusability of the biosensor, thus avoiding the nanostructures collapse on the gold sensing surface.

The employment of NSs in the labeled sandwich-like assay reduced the detection limits of about three orders of magnitude (from 6.1 nM to 10 pM) for a synthetic DNA target (84 mer). The strategy was successfully applied also to the detection of human genomic DNA pretreated with a tuned ultrasonication (Ermini et al., 2013), down to 6.9 aM, putting this result at the forefront of ultrasensitive detection in this field. In perspective, the developed ultrasensitive strategy could be possibly tested also for the direct detection of in-trace genetic material (*e.g.* oligonucleotidic biomarker) directly from biological samples (cell-free nucleic acid, ng/ml) in 'liquid biopsy', fast and helpful diagnostic tool for less invasive and fast clinical applications (Schwarzenbach et al., 2011).

Acknowledgments

The authors would like to thank Dr. Sandra Casale Laboratoire de Réactivité de Surfaces, Université Pierre & Marie Curie – Paris VI for the TEM image of gold nanostars.

Appendix A. Supplementary material

Supplementary data associated with this article can be found in the online version at:
http://dx.doi.org/10.1016/j.bios.2015.07.071.

References

Bedford, E.E., Spadavecchia, J., Pradier, C., Gu, F.X., 2012. Macromol. Biosci. 16, 724–739.
D'Agata, R., Breveglieri, G., Zanoli, L.M., Borgatti, M., Spoto, G., Gambari, R., 2011. Anal. Chem. 83, 8711–8717.
Daniel, M.-C., Astruc, D., 2004. Chem. Rev. 104 (1), 293–346.
D'Agata, R., Spoto, G., 2013. Anal. Bioanal. Chem. 405, 573–584.
Ermini, M.L., Mariani, S., Scarano, S., Minunni, M., 2013. Biosens. Bioelectron. 40, 193–199.
Hao, F., Nehl, C.L., Hafner, J.H., Nordlander, P., 2007. Nano Lett. 7, 729–732.
Homola, J., 2008. Chem. Rev. 108, 462–493.
Li, Y., Wark, A.W., Lee, H.J., Corn, R.M., 2006. Anal. Chem. 78, 3158–3164.
Nelson, B.P., Grimsrud, T.E., Liles, M.R., Goodman, R.M., Corn, R.M., 2001. Surface plasmon resonance imaging measurements of DNA and RNA hybridization adsorption onto DNA microarrays. Anal. Chem. 73, 1–7.
Mariani, S., Minunni, M., 2014. Anal. Bioanal. Chem. 406, 2303–2323.
Mariani, S., Scarano, S., Carrai, M., Barale, R., Minunni, M., 2015a. Anal. Bioanal. Chem. 407 (14), 4023–4028.
Mariani, S., Scarano, S., Ermini, M.L., Bonini, M., Minunni, M., 2015b. Chem. Commun. 51, 6587–6590.
Marzolini, C., Paus, E., Buclin, T., Kim, R.B., 2004. Clin. Pharm. Ther. 75, 13–33.
Mirkin, C.A., Letsinger, R.L., Mucic, R.C., Storhoff, J.J., 1996. Nature 382, 607–609.
Scarano, S., Mascini, M., Turner, A.P.F., Minunni, M., 2010a. Biosens. Bioelectron. 25, 957–966.
Scarano, S., Scuffi, C., Mascini, M., Minunni, M., 2010b. Biosens. Bioelectron. 26, 1380–1385.
Schwarzenbach, H., Hoon, D.S.B., Pantel, K., 2011. Nat. Rev. Cancer 11, 426–437.
Shi, L., Perkins, R.G., Fang, H., Tong, W., 2008. Curr. Opin. Biotechnol. 19, 10–18.
Šípová, H., Homola, J., 2013. Anal. Chim. Acta 773, 9–23.
Spadavecchia, J., Barras, A., Lyskawa, J., Woisel, P., Laure, W., Pradier, C.-M., Boukherroub, R., Szunerits, S., 2013. Anal. Chem. 85, 3288–3296.
Spadavecchia, J., Casale, S., Landoulsi, J., Pradier, C.-M., 2014. Chem. Phys. Lett. 609, 134–141.
Spoto, G., Corradini, R. (Eds.), 2012. Detection of Non-amplified Genomic DNA. Springer, Germany.
Spoto, G., Minunni, M., 2012. Phys. Chem. Lett. 3, 2682–2691.
Špringer, T., Ermini, M.L., Špačková, B., Jabloňků, J., Homola, J., 2014. Anal. Chem. 86, 10350–10356.
Steiner, G., 2004. Anal. Bioanal. Chem. 379, 328–331.
Szunerits, S., Spadavecchia, J., Boukherroub, R., 2014. Rev. Anal. Chem. 33 (3), 153–212.
Tan, S.J., Campolongo, M.J., Luo, D., Cheng, W., 2011. Nat. Nanotechnol. 6, 268–276.
Wernersson, R., Juncker, A.S., Nielsen, H.B., 2007. Nat. Protoc. 2, 2677–2691.
Zagorodko, O., Spadavecchia, J., Serrano, A.Y., Larroulet, I., Pesquera, A., Zurutuza, A., Boukherroub, R., Szunerits, S., 2014. Anal. Chem. 86, 11211–11216.
Zanoli, L.M., Agata, R.D., Spoto, G., 2012. Anal. Bioanal Chem. 402, 1759–1771.